Lobo, F. J. y Ridente, D. 2013. Milankovitch cyclicity in modern continental margins: stratigraphic cycles in terrigenous shelf settings. *Boletín Geológico y Minero,* 124 (2): 169-185
ISSN: 0366-0176

Milankovitch cyclicity in modern continental margins: stratigraphic cycles in terrigenous shelf settings

F. J. Lobo[(1)] y D. Ridente[(2)]

(1) Instituto Andaluz de Ciencias de la Tierra (CSIC-Universidad de Granada), Avenida de las Palmeras nº 4, 18100 Armilla, Spain
(2) Istituto di Geologia Ambientale e Geoingegneria (CNR-IGAG), c/o Sapienza Università di Roma, P.le Aldo Moro 5, 00185 Rome, Italy.

ABSTRACT

We present a synthesis of the sedimentary responses to Late Quaternary Milankovitch-type sea-level cycles (100 and 20 kyr periodicities) as a basis for our investigations into the patterns and concepts of composite sequences in shallow-shelf settings. We describe the record of both 100 and 20 kyr cycles as documented worldwide and discuss the pattern of composite cyclicity mainly on the basis of previously published data from the Adriatic Sea and Gulf of Cádiz margins. Cycles of 100 kyr are those most frequently documented in Quaternary margins; they occur in the form of unconformity-bounded depositional sequences dominated by fairly uniform progradational-regressive units and more variable, though less well developed, transgressive deposits. Sequence boundaries correspond to prominent polygenic (regressive-transgressive) erosional surfaces that bear witness to considerable transgressive reworking of the original sub-aerial unconformity. Although the progradational units making up the greater part of these sequences have usually been interpreted as a record of a falling sea-level stage, recent evidence is pointing towards a more complex stratigraphic picture, including a distinction between relative highstand and lowstand deposits. The 20-kyr stratigraphic motifs show greater variation compared to that displayed by the more common 100-kyr sequences, particularly in the basic structure of systems tracts and the nature of bounding surfaces. The two case studies described here, the Adriatic Sea and Gulf of Cádiz margins, highlight the fact that, concomitantly with an increase in frequencies of cycles and sequences, sediment supply and the dynamics of their dispersal significantly affected the stratigraphic response to the main controlling factor, which was sea-level, thus determining the variety of expression in the 20 kyr cycles.

Key words: Adriatic, composite cycles, Gulf of Cádiz, Quaternary, sequence stratigraphy

El registro de la ciclicidad de Milankovitch en márgenes continentales actuales: ciclos estratigráficos en plataformas terrígenas

RESUMEN

Una síntesis de las respuestas sedimentarias a los ciclos del nivel del mar del Cuaternario terminal de la banda de Milankovitch se presenta en esta contribución, como base para investigar los patrones y conceptos de secuencias compuestas en ambientes someros de plataforma. Tras describir el registro de ciclos de 100 y 20 kyr descritos a nivel global, se discute el patrón de ciclicidades superimpuestas de dos márgenes como el Mar Adriático y el Golfo de Cádiz.

Los ciclos de 100 kyr son los más documentados en márgenes cuaternarios; se presentan bajo la forma de secuencias deposicionales limitadas por discontinuidades y compuestos mayoritariamente por unidades progradantes regresivas y depósitos transgresivos que muestran un menor desarrollo y mayor variabilidad. Los límites de secuencias se corresponden con superficies de erosión poligenéticas (regresivas-transgresivas) que reflejan un retrabajamiento transgresivo significativo de la discontinuidad subaérea original. Aunque las unidades progradantes que edifican en gran medida las secuencias han sido consideradas como resultado fundamental del descenso del nivel del mar, evidencias recientes están dilucidando una arquitectura estratigráfica más compleja, que permite la determinación de depósitos generados bajo condiciones de estabilización del nivel del mar.

Las alternancias estratigráficas asociadas a la ciclicidad de 20 kyr muestran una mayor variabilidad que las secuencias de 100 kyr, particularmente en la estructura básica de cortejos sedimentarios y la naturaleza de superficies limitantes. Los dos ejemplos descritos (Mar Adriático y Golfo de Cádiz) resaltan el hecho de que, *en consonancia con el incremento de frecuencias de ciclos y secuencias, el aporte sedimentario y la dinámica de dispersión del sedimento afectan de una manera significativa la respuesta estratigráfica al factor de control principal (nivel del mar), determinando de esta forma una expresión variada de los ciclos de 20 kyr.*

Palabras clave: Adriático, ciclos compuestos, Cuaternario, estratigrafía secuencial, Golfo de Cádiz

VERSION ABREVIADA EN CASTELLANO

Introducción y metodología

La ciclicidad de Milankovitch determina que las variaciones de radiación solar ejercen una influencia significativa en el crecimiento y retracción de láminas de hielo permanentes, modificando de esta forma los volúmenes globales del océano. Dicha ciclicidad puede ser determinada fundamentalmente a partir del registro de la variación del isótopo de oxígeno O^{18}. La dificultad de correlacionar la estratigrafía de ambientes profundos (donde se detecta el registro de O^{18}) con las unidades deposicionales de plataforma (donde las fluctuaciones del nivel del mar modelan directamente la arquitectura deposicional) ha limitado significativamente la posibilidad de determinar la influencia de los diferentes ciclos de Milankovitch (con periodicidades variables desde decenas a centenas de miles de años) en el registro de los márgenes continentales.

Las secuencias deposicionales que registran los ciclos de Milankovitch son consideradas de alta frecuencia. Su desarrollo y preservación potencial se favorecen en áreas con tasas elevadas de sedimentación y subsidencia, como las plataformas continentales. Estas áreas pueden ser investigadas por medios de técnicas de prospección de alta resolución, lo cual permite desvelar las diferentes escalas y jerarquías de los ciclos globales del nivel del mar. De esta forma, los márgenes continentales cuaternarios se consideran ambientes ideales para estudiar el control de los cambios globales del nivel del mar en la organización interna de las secuencias deposicionales y la naturaleza compuesta de la ciclicidad de alta frecuencia. Existen dos tipos principales de secuencias deposicionales de alta frecuencia cuaternarias controladas por los ciclos de Milankovitch (100 y 20 kyr), que determinan dos ciclos de variación del nivel del mar durante el Cuaternario. Los ciclos de 100 kyr han sido identificados para los últimos 800 kyr, y vienen controlados por los cambios mayores de volumen de hielo que definen períodos de descenso gradual del nivel del mar y subidas abruptas tras los máximos glaciares. Los ciclos de 20 kyr se han descrito en los últimos 250 kyr, y también presentan un carácter asimétrico (Fig. 1).

La representación y significación estratigráfica de dichos ciclos ha sido y permanece discutida en la actualidad. Dichas secuencias también muestran diferencias con el modelo secuencial de baja resolución, así como con el patrón jerárquico de secuencias deposicionales definido en el registro fósil. Teniendo en cuenta estos factores, pretendemos definir de que forma la superposición de ciclos de Milankovitch queda reflejada en el registro cuaternario de plataformas, por medio de: 1) la definición de cortejos sedimentarios que componen las secuencias deposicionales de 100 kyr; 2) la relación de los diferentes cortejos de las secuencias de 100 kyr con las oscilaciones del nivel del mar de 20 kyr que modulan la ciclicidad de 100 kyr; 3) la definición de superficies estratigráficas por medio de las cuales unidades internas de las secuencias de 100 kyr pueden ser consideradas como secuencias de mayor frecuencia.

El estudio de dichas ciclicidades y su registro en los medios someros marinos normalmente se ha realizado por medio de la correlación de la arquitectura deposicional de las secuencias reconocida por medio de perfiles sísmicos de alta resolución con análisis sedimentológicos de detalle y dataciones que proporcionan información de los ambientes sedimentarios y un marco cronoestratigráfico donde las diferentes secuencias pueden ser emplazadas.

Resultados y discusión

Los ciclos de 100 ka están representados por secuencias deposicionales limitadas por discontinuidades erosivas, y compuestos en gran medida por cortejos sedimentarios progradantes generados durante los descensos del nivel del mar, aunque pueden contener también cortejos sedimentarios de alto nivel del mar. Por el contrario, los depósitos transgresivos muestran espesores reducidos y extensiones laterales limitadas (Fig. 2).

Las arquitecturas estratigráficas asociadas a los ciclos de 20 kyr muestran una mayor variabilidad espacio-temporal, aunque los depósitos regresivos asociados a los descensos del nivel del mar también son dominantes (Fig. 3). De forma particular, los depósitos transgresivos muestran una representación muy variable en función de las condiciones oceanográficas. Asimismo, se observa una variación temporal de las facies en las secuencias asociadas a los ciclos de 20 kyr desde el último interglaciar hasta el último máximo glaciar, ya que los depósitos litorales y deltas dominados por el oleaje tienden a ser substituidos por deltas de borde de plataforma.

En algunos medios de plataforma actuales se han identificados los dos tipos de ciclicidades. Entre ellos, destacan los ejemplos del Mar Adriático (Mar Mediterráneo) y el Golfo de Cádiz (Océano Atlántico). En la plataforma Adriática, se han identificado 4 secuencias deposicionales de 100 ka las cuales han sido muestreadas en un sondeo de 71 m de profundidad extraído en el talud superior. A partir de ello, se determina que las secuencias de 100 ka están internamente compuestas por unidades progradantes, que se suceden en respuesta a la variación del nivel del mar de alta frecuencia que modula los ciclos de 100 ka. Específicamente, dichas unidades internas parecen reflejar la alternancia de depósitos de alto nivel del mar y depósitos regresivos/de bajo nivel del mar, cuyos límites no muestran un carácter marcadamente erosivo (Fig. 4).

En el Golfo de Cádiz también se han detectado dos escalas estratigráficas (Fig. 5), aparentemente relacionadas con las dos ciclicidades dominantes (100 y 20 ka) (Fig. 6). A diferencia del Mar Adriático, en este caso, las dos escalas de secuencias muestran semejanzas significativas. Ambas están dominadas por unidades progradantes que incrementan su espesor hacia la cuenca, entre las cuales se intercalan unidades laminares con configuraciones internas subparalelas. Las unidades progradantes muestran truncaciones erosivas a techo en las dos escalas de secuencias.

En relación con la arquitectura interna de las secuencias de 100 ka, las tendencias recientes tratan de definir con detalle la arquitectura progradacional desde condiciones de alto nivel a bajo nivel. En determinados ambientes, el límite alto nivel-regresivo se identifica como una superficie de downlap, bajo condiciones favorables de subsidencia y/o de aporte sedimentario suficiente que permite la generación de depocentros distales. El reconocimiento del límite regresivo-bajo nivel es más difícil, ya que solo parece evidente en ambientes caracterizados por un incremento de las condiciones energéticas en función de la bajada del nivel del mar.

Aunque en la mayor parte de los ambientes de plataforma una ciclicidad aparece como dominante, en determinadas áreas se identifican las dos ciclicidades. En estos casos, el patrón compuesto se detecta en el interior de la sucesión de cuñas progradantes que registran el descenso general del nivel del mar entre cada período interglaciar y glacial. De acuerdo con el modelo conceptual de alta resolución, dichas unidades progradantes constituirían secuencias individuales que formarían un conjunto de secuencias. En dicho modelo, esos conjuntos de secuencias podrían desarrollarse durante el ciclo completo de variación del nivel del mar. Esa diferencia es atribuida al patrón asimétrico de las fluctuaciones del nivel del mar que es dominante durante el Cuaternario.

Las evidencias provenientes de varios ambientes de plataforma, incluyendo el Mar Adriático y el Golfo de Cádiz, indicarían que las unidades estratigráficas asociadas a los ciclos de 20 ka muestran diferencias significativas en términos de de naturaleza de superficies limitantes y patrón general de clinoformas (Figs. 4 y 6). Esas diferencias indicarían que diversos factores como la subsidencia regional, el aporte sedimentario y el patrón de dispersión del sedimento pueden modificar de una forma muy importante la expresión estratigráfica de los ciclos de 20 ka que se superponen a los ciclos de 100 ka. Específicamente, los límites entre las unidades pueden variar entre nítidamente erosivos en algunas áreas como el Golfo de Cádiz, donde podrían ser considerados límites de secuencias, a otras zonas como el Mar Adriático donde los límites no se pueden trazar con claridad, y esa ciclicidad de alta frecuencia viene expresada en gran medida por variaciones de la configuración de las unidades.

Introduction

According to the hypothesis formulated in the past century by Milankovitch (1930), climate cycles are controlled by variations in the earth's orbital geometry, reflected in precession, obliquity and eccentricity; these variations modulate changes in solar radiation during individual cycles of about 20, 40 and 100 kyr. These variations in solar radiation have exerted a considerable influence upon the growth and decay of permanent ice sheets, thereby modifying global ocean volumes (Chappel, 1974). Milankovitch cyclicity was first detected in the marine geological record by recognising past variations in the ocean's oxygen-isotope composition (Emiliani, 1955; Shackleton and Opdyke, 1973), on the basis of which Hays *et al.* (1976) went on to use the sedimentary record of deep oceans to assess oxygen-isotope variation ($\delta^{18}O$) and reconstruct sea-level curves relating to past climate changes (see the SPECMAP curve). Difficulties involved in correlating deep-sea stratigraphy, in which the $\delta^{18}O$ record of cyclicity is detectable, with depositional units on continental shelves, where sea-level fluctuations directly shape sequence architecture, have significantly limited the possibility of determining how and to what extent the contribution of each individual cycle is reflected in the stratigraphic record of continental margins (Ridente *et al.*, 2008).

Depositional sequences recording Milankovitch cyclicity are regarded as "high-frequency" sequences, as opposed to "low-frequency" sequences responding to global sea-level cycles controlled by factors other than astronomically-induced climate change and generally spanning millions of years. On this basis, cycles and sequences are classified in "orders" of growing rank from lower to higher frequencies (Mitchum and Van Wagoner, 1991). Milankovitch cycles typically produce 4^{th} and 5^{th} order sequences, spanning 100-200 kyr and 10-40 kyr intervals respectively (Mitchum and Van Wagoner, 1991; Vail *et al.*, 2002). The potential development and preservation of high-frequency sequences are favoured in areas with high sedimentation rates and comparable rates of subsidence (Mitchum and Van Wagoner, 1991). Modern shallow-shelf settings generally meet those requirements, besides which, because of their shallow depth, Quaternary sequences in modern continental margins can be imaged by means of very-high-resolution seismic profiles that allow us to unravel depositional (seismic) units reflecting the different scales and hierarchy of global sea-level cycles. Quaternary continental margins are thus ideal contexts for investigating the control of global sea level upon the internal organisation of depositional sequences and the composite nature of high-frequency cyclicity.

The wide application of high-resolution techniques during the past two decades has revealed that Quaternary depositional sequences typically reflect the dominance of one main Milankovitch cycle, although there is still debate about the representation and stratigraphic significance of 100 kyr versus 20 kyr sequences (Kolla *et al.*, 2000; Rabineau *et al.*, 2005; Bassetti *et al.*, 2008; Ridente *et al.*, 2009). Moreover, sequences reflecting high-frequency cycles show some significant differences with regard to the basic stratigraphic sequence model, deriving largely from low-frequency sequences (Yoo and Park, 2000). These departures also include differences between the Quaternary record of composite Milankovitch cycles and the hierarchical pattern proposed by Mitchum and Van Wagoner (1991), according to which composite sequences occur in the sedimentary record in a fractal pattern.

Objectives

We review here the existing published data in order to compare the distinctive attributes of 4th and 5th order stratigraphic units (sequences and systems tracts) related to Quaternary 100 and 20 kyr glacio-eustatic cycles. These units sculpt the most recent stratigraphic intervals in many terrigenous shallow-water settings and reflect the relative importance of different controlling factors at the scale of the two main cycles. On the basis of two case studies, those of the Adriatic Sea and the Gulf of Cádiz, we try to demonstrate how composite cyclicity modulates the stratigraphic record, a key issue for: 1) defining distinct systems tracts (LST: lowstand systems tract; TST: transgressive systems tract; HST: highstand systems tract; FSST: falling-stage systems tract) within the overall self-similar set of progradational units that typically compose 100 kyr sequences; 2) relating distinct systems tracts within 100 kyr sequences to specific intervals of the 20 kyr sea-level oscillations that punctuate the dominant 100 kyr cyclicity; and 3) defining stratigraphic surfaces by which internal units within 100 kyr sequence can be classified as sequences on the scale of the 20 kyr cycle.

Background: the patterns of Quaternary sea-level change

Emerged coral records, indicative of palaeo-sea levels, have been used in conjunction with $\delta^{18}O$ benthic isotope records, a proxy of changes in ocean volume, to define Quaternary changes in sea level (Imbrie *et al.*, 1984). Additional indications of sea level changes have been provided by geomorphological, stratigraphic and palaeontological evidence from coastal to upper-slope environments, which are very sensitive to these changes (Cronin, 1983). Nevertheless, estimates of the amplitude of sea-level oscillations may differ significantly. Uncertainties have in the past been particularly affected by the implications of ice volume and, by extension, the magnitudes of sea-level changes as derived from the deep-sea $\delta^{18}O$ record. A number of improvements closed the gap between reef-derived sea levels and the deep-ocean isotope record, including the removal of temperature and hydrological effects in $\delta^{18}O$ data (Shackleton, 1987; Lea *et al.*, 2002), and more precise measurements of the age of emerged reef terraces (Chappell *et al.*, 1996). Most of the observations document the dominant imprint of 100 kyr cyclicity in Quaternary continental margins, although there are cases where the basic sequence architecture seems to respond to the 20 kyr beat (references provided in the chapter devoted to higher-order sequences). On the other hand, sequences predating the Middle Pleistocene, more extensively known through outcrops on land, point to a prevailing control by 40 kyr cyclicity during the Pliocene and Early Pleistocene (Naish and Kamp, 1997; Massari *et al.*, 1999; Kitamura *et al.*, 2000).

100 kyr sea-level fluctuations

Spectral analysis of Quaternary $\delta^{18}O$ records, ordered into marine isotope stages and sub-stages (MISs), provided the strongest support for the assumption that the observed ca. 100 kyr sea-level changes matched the average duration of the orbital eccentricity cycle (Hays *et al.*, 1976); since then, increasing evidence has been put forward by the SPECMAP Project (Martinson *et al.*, 1987; Imbrie *et al.*, 1993; Petit *et al.*, 1999), leading to a general consensus of opinion that the 100-ka cycle represents the expression of major changes in ice volume (Fig. 1).

The 100 kyr cyclicity, as reflected in the geological record, is clearly indicative of the more extreme glacial events during the last ca. 800 kyr, with greater impacts on the amplitude of sea-level changes (Shackleton, 1997; Raymo *et al.*, 1997). The timing and duration of maximum ice-cap expansion and decay exerts a primary influence on the establishment of 100 kyr sea-level cycles (Martinson *et al.*, 1987; Ruddiman, 2003). These cycles are characterised by slow phases of sea-level fall, marking a progressive cooling leading to glacial lowstands, followed by rapid, high-amplitude (> 100 m), interglacial sea-level rises known as terminations (Fig. 1). During the last 800 kyr glacial terminations culminated in the interglacial sea-level highstands of MISs 19, 17, 15, 13, 11, 9, 7, 5 and 1. Interglacial highstands differed in amplitude, duration and nature, some of them showing single peaks whilst others have multiple peaks (Siddall *et al.*, 2007). On the basis of oxygen-isotope records, short-lived (about 10% of the cycle duration) maximum lowstand phases during glacial acmes have been reported for the last 500 kyr, dating back at least to MIS 12 (Rohling *et al.*, 1998). These sea-level lowstands witnessed sea-level drops of 120-140 m below present levels (Rohling *et al.*, 1998; Lea *et al.*, 2002; Waelbroeck *et al.*, 2002) (Fig. 1). The long-lived falling phase of the 100 kyr cycle (up to 70-80% of the cycle duration) is unsteady because of the superposition of 20 kyr cycles, thus generating a record of composite cyclicity for the Quaternary that is difficult to disentangle on the basis of theoretical concepts alone (Mitchum and Van Wagoner, 1991).

20 kyr sea-level fluctuations

Evidence of 20 kyr sea-level cycles can be found in the stratigraphic record extending back to MIS 8 (Lea *et al.*, 2002; Waelbroeck *et al.*, 2002), although they are clearest for the interval between MIS 6 and MIS 2, during which sea-level highstands occurring at roughly 20 kyr intervals have been dated at 130-120 (last interglacial), 105-97, 88-80, 60, 50-40 and 30-28 ka (Bloom *et al.*, 1974; Williams *et al.*, 1981; Bard *et al.*, 1990). These sea-level maxima would correspond to MISs

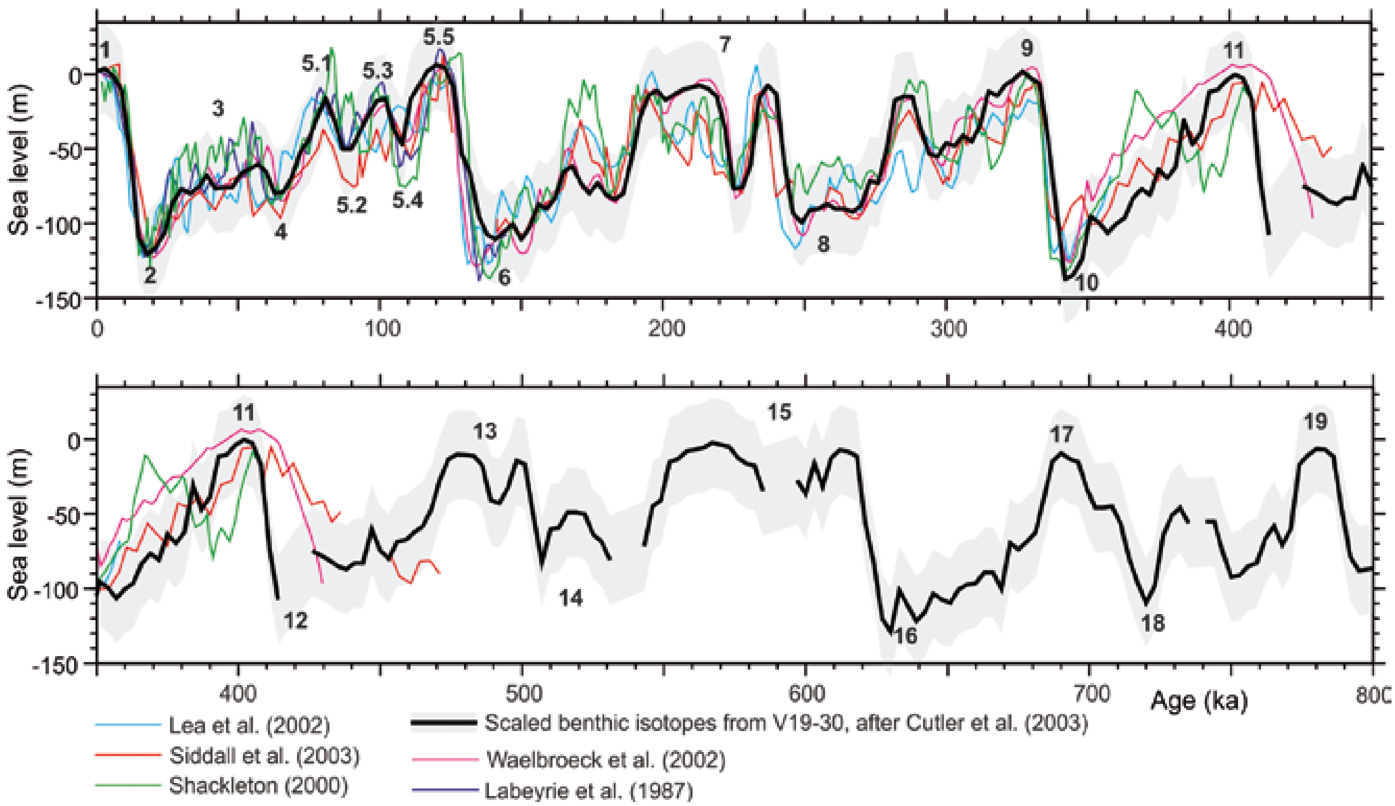

Figure 1. Sea-level estimates for the last 800 kyr obtained from different oxygen-isotope sources. Marine isotope stages are numbered. Modified from Siddall *et al.* (2007).

Figura 1. *Estimaciones del nivel del mar para los últimos 800 kyr obtenidas de diferentes curvas de isótopos de oxígeno. Los estadios isotópicos marinos aparecen numerados. Modificada a partir de Siddall* et al. *(2007).*

5.5, 5.3, 5.1 and to several peaks during MIS 3, and the alternating sea-level minima to MISs 5.4, 5.2, 4, intra-MIS 3 and MIS 2 (Williams *et al.*, 1981) (Fig. 1). Within the last ca. 350 kyr, deposits recording 20 kyr cycles match the relative highstand intervals marking MISs 9, 7 and 5, and less frequently they are superimposed upon intervals of lower sea level such as MISs 6 and 3 (Gallup *et al.*, 1994; Lea *et al.*, 2002; Waelbroeck *et al.*, 2002) (Fig. 1).

As in the case of the 100 kyr cycle, but on a smaller scale, the shape of the 20 kyr sea-level curve is asymmetric, with relatively longer phases of sea-level fall, reflecting slow ice-sheet growth and shorter sea-level rises induced by more rapid ice disintegration and meltwater pulses (Siddall *et al.*, 2010; Yokoyama and Esat, 2011).

The record and architecture of high-frequency sequences

The stratigraphic record of 100 kyr cycles

One of the first indications that stacked sets of depositional sequences in Quaternary continental margins could be correlated with the 100 kyr signature of $\delta^{18}O$ curves came from the Seyhan-Ceyhan delta system in the eastern Mediterranean (Piper and Aksu, 1992). Following these findings, 100 kyr cyclicity has been widely observed in Quaternary continental margins as consisting of stacks of multiple unconformity-bounded sequences. The set of sequences in the Seyhan-Ceyhan delta system has been correlated with isotope stages extending back to MIS 16 (ca. 600 kyr) and has served as a case study for defining the relationship between shelf-margin progradation and the amplitude of sea-level fall during 100 kyr cycles; less emphasis, however, has been given to the internal architecture of individual sequences forming there.

The internal architecture of Quaternary 100 kyr sequences has been particularly emphasised in the Gulf of Mexico, where the seismic-stratigraphic reconstruction of the past 130 kyr sequence bears witness to the dominance of falling-sea-level deposits (i.e. forced-regression deposits; *cf.* Plint, 1991) over highstand and lowstand progradation (Sydow and Roberts, 1994). Examples of similar regressive sequences have been reported in several margins in the Mediterranean and nearby areas, such as the Gulf of Lion (Tesson *et al.*, 2000; Rabineau *et al.*, 2005), the western Adriatic margin (Trincardi and Correggiari, 2000), the Tyrrhenian margin (Chiocci, 2000; Ridente *et al.*, 2012), the Rhone Delta (Tesson *et al.*, 2000), the NE (Liquete *et al.*, 2008) and SW (Somoza *et al.*, 1997; Hernández-Molina *et al.*, 2000) Spanish margins, the Aegean Sea (Ulug *et al.*, 2005) and the Marmara Sea (Çağatay *et al.*, 2009). Outside the Mediterranean, 100 kyr sequences recording shelf-margin progradation have been reported in the Asiatic region off the Korean coast (Yoo *et al.*, 2003), the East (Berné *et al.*, 2002) and South China Sea (Hiscott, 2001) and off the Californian seaboard (Burger *et al.*, 2002) and in the New Jersey Atlantic continental margin in N. America (McHugh and Olson, 2002).

The above examples provide evidence that 100 kyr sequences of the past 500-600 kyr from diverse settings are typically asymmetric in shape and depositional architecture, being composed essentially of overall progradational deposits and to a lesser extent by aggradational units (Fig. 2). There is a dearth of chronostratigraphic evidence but these progradational units are regarded generically as being forced-regression deposits during a falling phase, although they may include relative highstand units formed after major terminations or during the lower-amplitude sea-level rises and highstands that punctuate the long-term sea-level fall. Even more difficult is the recognition of transgressive units, which, within 100 kyr sequences, are typically thinner and limited in their lateral extent (Hernandez-Molina *et al.*, 2000; Lobo *et al.*, 2002; Hanebuth *et al.*, 2002; Ridente *et al.*, 2008).

The stratigraphic record of 20 kyr cycles

The existence of more frequent depositional sequences than those of the dominant 100 kyr pacing has been inferred in several margins, although their stratigraphic expression varies considerably from place to place. The following stratigraphic patterns have been depicted: (a) Two major erosional surfaces interpreted as being sequence boundaries related to the two major lowstands during MISs 4 and 2. These boundaries top two major progradational intervals during MISs 5-4 and 3-2 in response to sub-aerial erosion and subsequent transgressive ravinement (Osterberg, 2006; Çağatay *et al.*, 2009); (b) Multiple progradational events during MISs 5-4. This scheme is based on the identification of 2-3 cycles of coastal-to-shelf progradation (normally of prodeltaic origin) motivated by 20 ka oscillations within MIS 5 (Somoza *et al.*, 1997; Hernández-Molina *et al.*, 2000; Hiscott, 2001; Abdulah *et al.*, 2004; Banfield and Anderson, 2004; Liu *et al.*, 2010). The MIS 3-2 interval is represented by a single shelf-edge deltaic lobe capped by a prominent erosional surface (Hiscott, 2001; Abdulah *et al.*, 2004; Liu *et al.*, 2010); (c) Multiple progradational events during MISs 3-2. Sequences occur in relation to intra-MIS

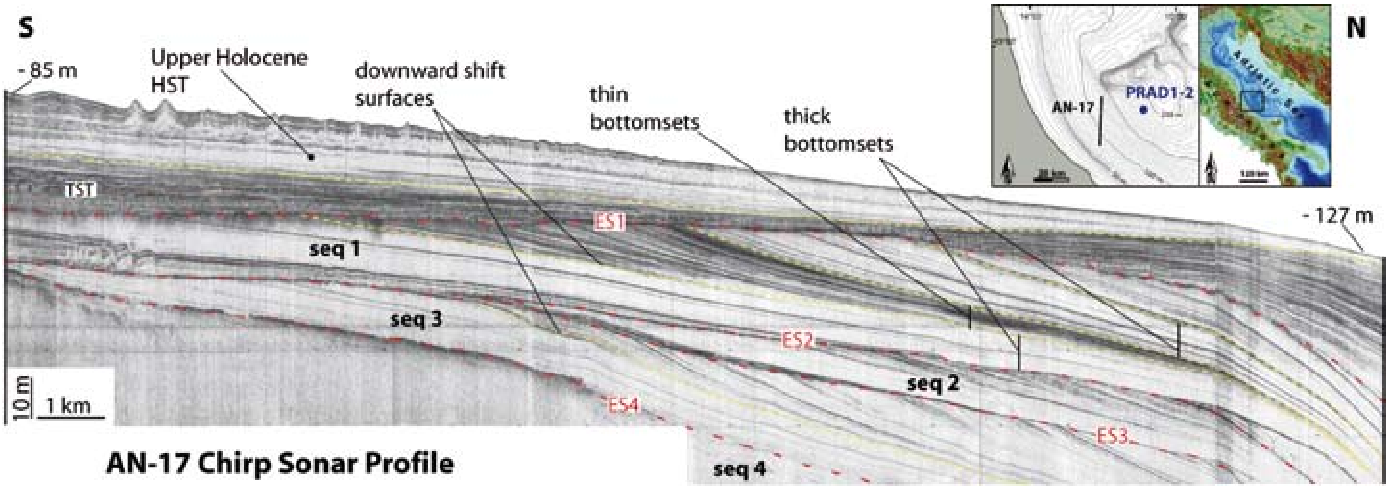

Figure 2. Seismic profile showing the record of 100 kyr sequences (sequence 1 to 4, top-down) internally composed of progradational clinoforms in the western Adriatic shelf. Sequence boundaries correspond to erosional unconformities (ES 1 to ES 4) on the shelf (dashed red lines); internal progradational units are separated by regressive marine-erosion surfaces (dashed yellow lines) locally marking an abrupt contact between overlying progradational foresets downlapping flatter/thicker bottomsets (downward shift surfaces) of previous progradational units. Upper Pleistocene-Lower Holocene transgressive (TST) and upper Holocene highstand (HST) units are also shown. The location map indicates the site of the PRAD 1-2 borehole, where marine isotope stages and sub-stages over the past ca. 400 kyr have been reconstructed. Legend: TST: transgressive systems tract; HST: highstand systems tract. Modified from Ridente *et al.* (2008).

Figura 2. *Perfil sísmico que muestra el registro de las secuencias de 100 kyr (secuencia 1 a 4 de techo a muro) compuestas internamente por clinoformas en el margen occidental del Mar Adriático. Los límites de secuencia están representados por discontinuidades erosivas (ES1 a ES 4) en la plataforma (líneas rojas discontinuas); las unidades progradantes internas están separadas por superficies regresivas de erosión marina (líneas discontinuas amarillas), que marcan localmente contactos abruptos (superficies de cambio hacia la cuenca) entre foresets progradantes sobre bottomsets menos inclinados y más potentes de unidades progradantes previas. Se muestran asimismo las unidades transgresivas (TST) del Pleistoceno Superior-Holoceno Inferior y las unidades de alto nivel del mar (HST) del Holoceno Superior. El mapa de localización incluye la posición del sondeo PRAD 1-2, a partir del cual se han reconstruido los estadios (y sub-estadios) isotópicos marinos para los últimos 400 kyr. Leyenda: TST: Cortejo Sedimentario Transgresivo; HST: Cortejo Sedimentario de Alto Nivel del Mar. Modificado a partir de Ridente* et al. *(2008).*

3 sea-level fluctuations (Marsset *et al.*, 1996; Liu *et al.*, 2000), with a single MIS 5 progradational event followed by the formation of an erosional bounding surface during MIS 4 (Liu *et al.*, 2000); (d) Multiple progradational events during the entire interval between MIS 6 and MIS 2. Sequences are separated by erosional unconformities (sequence boundaries) incised by fluvial channels formed during the relative lowstand pertaining to each 20 kyr cycle (Bellec and Cirac, 2010), although these unconformities are further reworked and modified by major fluvial incision during the extensive sub-aerial exposure concomitant with the MIS 2 lowstand, ultimately resulting in a major sequence boundary (Kolla *et al.*, 2000).

In general terms, these sequences are mainly composed of progradational (regressive) wedges interpreted as having been generated during a sea-level fall to lowstand, with a dominance of falling-stage (i.e. forced-regression) deposits (Kolla *et al.*, 2000; Jin *et al.*, 2002; Osterberg, 2006; Gámez *et al.*, 2009; Bellec and Cirac, 2010) (Fig. 3). In contrast to the overall uniformity of regressive intervals, transgressive phases show higher variability. The corresponding deposits are either missing or difficult to identify in many margins due to their relative thinness and limited lateral extension; in fact, they are typically represented by thin sheets or sparse channel-fill deposits (Abdulah *et al.*, 2004; Osterberg, 2006). In some cases, however, transgressive deposits show better development and/or preservation and occur as sub-parallel sheets (Bellec and Cirac, 2010), conspicuous tidal ridges (Marsset *et al.*, 1996; Liu *et al.*, 2000; Jin *et al.*, 2002) or in inner-shelf barrier-island settings (Ashley *et al.*, 1991).

Most frequently, a temporal evolution can be seen throughout the 20 kyr sequences that punctuate the 100 kyr cycle (Fig. 3). Intra-MIS 5 sequences tend to be composed of shore-face deposits and/or wave-dominated deltas. Fluvial incision is not significant, upward erosion is moderate and transgressive deposits are largely absent (Hiscott, 2001; Banfield and Anderson, 2004; Gámez *et al.*, 2009). In contrast, MISs 3 to 2 sequences show a preponderance of fluvial-dominated, shelf-margin deltas with oblique clinoforms prograding onto the shelf margin and upper slope (Banfield and Anderson, 2004; Gámez *et al.*, 2009). In addition, MISs 3-2 shelf-margin wedges are usually related to the cutting of major incised valleys during the sea-level fall (Kolla *et al.*, 2000; Hiscott, 2001; Liu *et al.*, 2010),

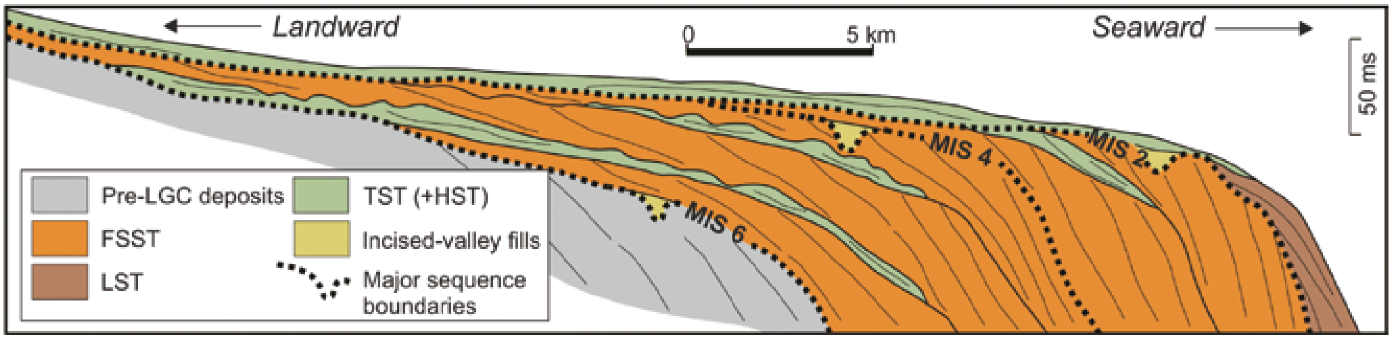

Figure 3. Synthetic stratigraphic interpretation of the last glacial cycle shelf architecture as being dominated by 20 kyr periodicity, which is considered to be representative of several North Atlantic settings, such as the Bay of Biscay, the Gulf of Cádiz and the Gulf of Mexico. Major erosional surfaces are related to the most pronounced lowstands (marine isotope stages (MISs) 6, 4 and 2). High-frequency sequences are dominated by falling-stage deposition (FSST), with enhanced lowstand deposits (LST) in the most recent interval. Other significant stratigraphic features include sheet-like transgressive deposition and incised-valley development in relation to major lowstands. Legend: LGC: last glacial cycle; FSST: falling-stage systems tract; LST: lowstand systems tract; TST: transgressive systems tract; HST: highstand systems tract. Synthetic profile constructed from stratigraphic interpretations included in Kolla *et al.* (2000), Hernández-Molina *et al.* (2000) and Bellec and Cirac (2010).

Figura 3. *Interpretación estratigráfica sintética de la arquitectura de la plataforma durante el Último Ciclo Glaciar, dominada por la periodicidad de 20 kyr que es considerada como representativa de varios ambientes someros del Atlántico Norte como el Golfo de Vizcaya, el Golfo de Cádiz y el Golfo de Méjico. Las superficies de erosión más significativas están asociadas a los intervalos de nivel del mar más pronunciados (Estadios Isotópicos Marinos 6, 4 y 2). Las secuencias de alta frecuencia muestran una composición dominada por depósitos de descenso del nivel del mar (FSST), con una mayor representación de los depósitos de bajo nivel del mar (LST) en la secuencia más reciente. Otros rasgos estratigráficos significativos incluyen la sedimentación transgresiva bajo la forma de láminas sedimentarias y el desarrollo de valles encajados durante los intervalos de bajo nivel del mar más importantes. Leyenda: LGC: Último Ciclo Glaciar; FSST: Cortejo Sedimentario de Descenso del Nivel del Mar; LST: Cortejo Sedimentario de Bajo Nivel del Mar; TST: Cortejo Sedimentario Transgresivo; HST: Cortejo Sedimentario de Alto Nivel del Mar. Perfil sintético construido a partir de las interpretaciones reflejadas en Kolla* et al. *(2000), Hernández-Molina* et al. *(2000) y Bellec y Cirac (2010).*

with a more frequent occurrence of fluvial deposition (Jin *et al.*, 2002).

Evidence of two architectural levels

A screening of the published data indicates that, depending on local deposition/preservation and available chronostratigraphic information, some settings reveal a stratigraphic complexity that can be interpreted in terms of composite (100 and 20 kyr) cyclicity. Amongst the most significant cases we describe examples from the Adriatic Sea and the Gulf of Cádiz, which provide useful insights into, firstly, how 20 kyr cycles shaped the internal architecture of the more common 100 kyr sequences, and secondly, what determined that, at least in some cases, the 20 kyr cycles themselves produced smaller-scale depositional sequences in the stratigraphic record. The following description derives mainly from published information, with the addition of some new seismic data and a subsequent interpretation of the eastern Algarve Shelf in the Gulf of Cádiz.

Adriatic Sea

The western Adriatic margin is built up of a set of four 100 kyr sequences, each displaying internal architecture consisting largely of progradational units in the order of a few to tens of metres thick (Fig. 2). Seismic stratigraphic analysis and numerical modelling have unveiled subtle but systematic variability in the downlap geometry and thickness of the foreset/bottomset region of the progradational units (Fig. 2; *cf.* Ridente and Trincardi, 2005). These were interpreted as reflecting changes in the amount of fine sediment supplied to the outer shelf through advection (Steckler *et al.*, 2007), a dispersal mechanism more efficient during highstand conditions and thus relatable to sea-level change (Cattaneo *et al.*, 2003).

The entire succession of sequence 1 to sequence 4 was recovered through a 71-m-long borehole (PRAD1-2, Fig. 2), drilled continuously in the upper slope (ca. 186 m water depth), where shelf clinoforms give way to regular and parallel seismic reflector packages (Ridente *et al.*, 2008). This allowed us to correlate directly the shelf progradational units with glacial-interglacial and stadial-interstadial intervals, as defined in borehole PRAD1-2, based on $\delta^{18}O$ records and eco-biostratigraphic proxies (Fig. 4). As a result, some of the progradational units previously conceived as being forced-regression units recording sea-level fall (Fig. 4a) could be put down to intervals of relative highstand (Fig. 4b) punctuating the overall 100 kyr sea-level fall (Ridente *et al.*, 2008). This refined stratig-

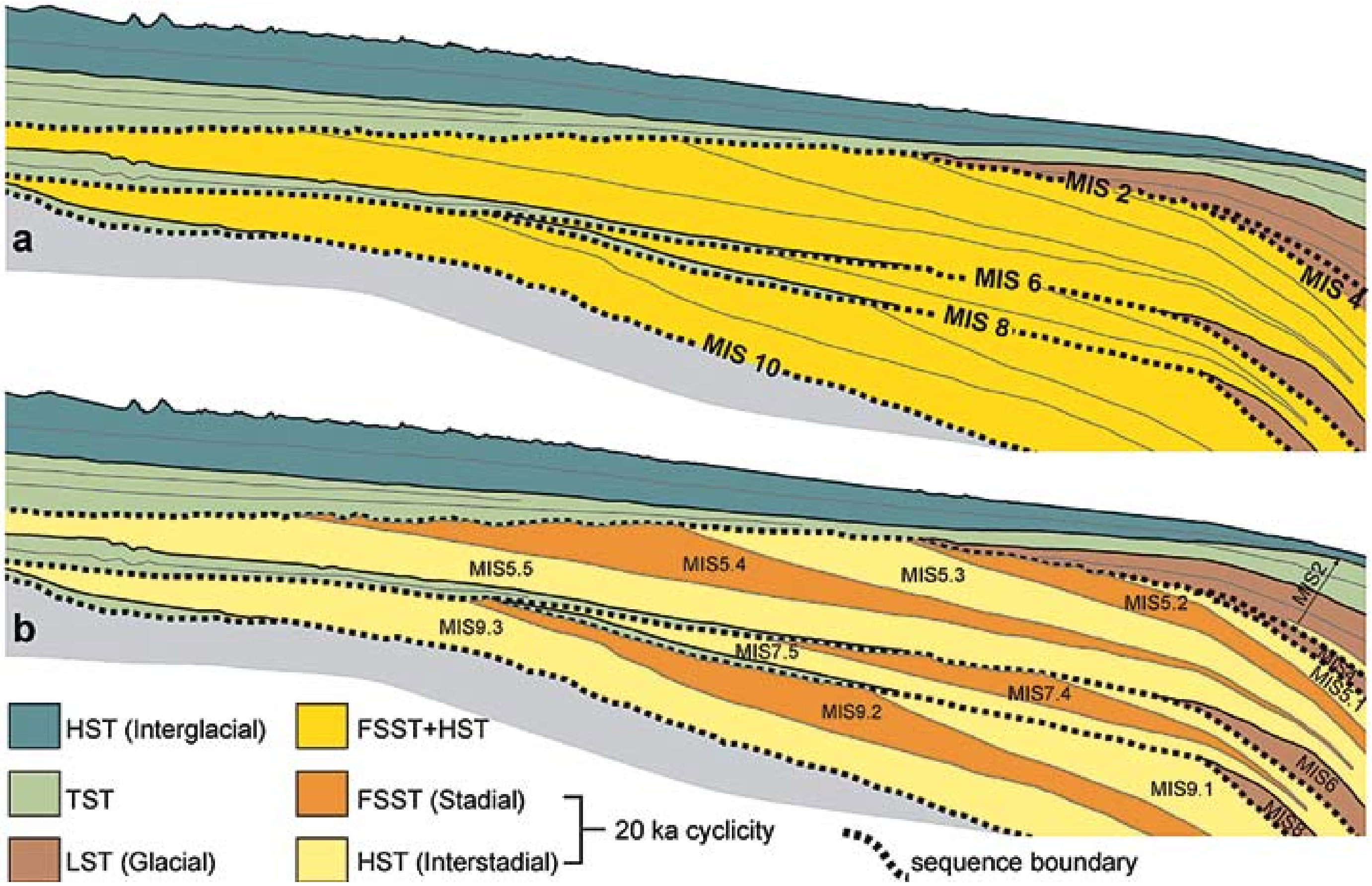

Figure 4. Sequence stratigraphic interpretations of the western Adriatic shelf architecture: (a) Line drawing based on seismic profile AN-17 (Fig. 2) showing evidence of 4[th] order (100 kyr) sequences with internal architecture characterized by indistinct progradational units recording highstand to lowstand sea levels within each depositional cycle; (b) Detailed internal architecture obtained by calibrating seismic stratigraphy with isotope stratigraphy derived from PRAD1-2. Interglacial and interstadial periods match progradational units displaying thicker-flatter bottomsets, typical of enhanced advection during highstand conditions. Stadials are recorded by progradational units with overall thinning bottomsets, indicating reduced sediment advection on the outer shelf during sea-level lowering. Note the reduced thickness of MIS 4 lowstand deposits, largely cannibalized (together with MIS 3 unit) by MIS 2 lowstand wedge. Legend: FSST: falling-stage systems tract; LST: lowstand systems tract; TST: transgressive systems tract; HST: highstand systems tract. Based on results from Ridente *et al.* (2008).

Figura 4. *Interpretaciones de estratigrafía secuencia del margen occidental del Mar Adriático: (a) esquema basado en el perfil sísmico AN-17 (Fig. 2) evidenciando secuencias de 4º orden (100 kyr) con una arquitectura interna caracterizada por unidades progradantes indiferenciadas registrando el segmento de variación del nivel del mar desde alto nivel hasta bajo nivel en cada ciclo deposicional. (b) Arquitectura interna de detalle obtenida a partir de la calibración de la estratigrafía sísmica con la estratigrafía isotópica derivada del sondeo PRAD1-2. Los períodos interglaciares e interestadiales se correlacionan con las unidades progradantes que muestran los bottomsets de menor inclinación y mayor espesor, característicos de procesos de advección favorecidos durante condiciones de alto nivel del mar. Los estadios isotópicos se registran por unidades progradantes que muestran un adelgazamiento global de los bottomsets, indicativo de una disminución de los procesos de advección en la plataforma externa durante los descensos del nivel del mar. A destacar el espesor reducido de los depósitos de bajo nivel del mar del estadio isotópico 4, los cuales fueron erosionados en su mayor parte (junto con la unidad del estadio isotópico 3) por la cuña de bajo nivel del mar asociada al estadio isotópico 2. Leyenda: FSST: Cortejo Sedimentario de Descenso del Nivel del Mar; LST: Cortejo Sedimentario de Bajo Nivel del Mar; TST: Cortejo Sedimentario Transgresivo; HST: Cortejo Sedimentario de Alto Nivel del Mar. Figura elaborada a partir de interpretaciones estratigráficas incluidas en Ridente* et al. *(2008).*

raphy provided direct evidence of how the variations observed in the downlap geometry and thickness of the bottomsets of shelf progradational units within sequences match the alternation of relative highstand and falling sea level punctuating 100 kyr cycles (Fig. 4). With reference to sequence 1, for instance, shelf progradational units displaying thicker and flatter bottomsets are those formed during the warmer MIS 5.5, MIS 5.3 and MIS 5.1, each interpreted as HST, recording intervals of relative highstand (compare Figs 2 and 4). Interposed progradational units with a clearer downlap geometry and thinner bottomsets (occasionally also presenting sharper basal surfaces, reflecting a more abrupt seaward shift of deposition) were formed during the cold intervals MIS 5.4, MIS 5.2 and MIS 4, each interpreted as FSST recording sea level fall (Fig. 4). Similarly, deposits encompassing MIS 7 and MIS 9 at site PRAD1–2 correlate in the shelf with sequences 2 and 3 respectively. Sequence 4 is seismically less clearly defined and its internal units could not be unravelled in terms of different systems tracts.

The pattern of variable HST and FSST progradational clinoforms described above is the most evident stratigraphic signature of the 20 kyr cyclicity superimposed on each 100 kyr depositional cycle, although, due to the lack of erosional surfaces separating HST-FSST couplets, a frame of smaller scale (5th order) unconformity-bounded sequences cannot be defined.

Gulf of Cádiz

To date, existing stratigraphic sequence models in the Gulf of Cádiz have not been dated directly. The observed architectures have instead been correlated with coastal highstand deposits exposed along the southern Iberian coast, with similar deposits found to the south of the gulf and in the nearby Alboran Sea, with the high-resolution stratigraphy of several Mediterranean shelves and with published Quaternary and Late Quaternary sea-level curves (Hernández-Molina *et al.*, 2000). Thus, in the shelf offshore the Guadiana River major depositional sequences have been related to 100 kyr cyclicity and a smaller-scale stratigraphic pattern has been primarily attributed to the influence of 20 kyr cycles (Somoza *et al.*, 1997). The two most recent 100 kyr depositional sequences display an asymmetric internal architecture due to the marked prevalence of units recording falling-lowstand versus rising-highstand sea levels.

A new, previously unpublished interpretation of seismic profiles collected in the Algarve Shelf to the west of the Guadiana River provides useful insights regarding the existence of composite sequences in the northern shelf of the gulf. The sedimentary stacking pattern is more clearly progradational than in the eastern shelf, enabling us to identify older sequences in the sedimentary succession (Fig. 5). This continental margin is dominated by wedge-shaped progradational units increasing in thickness seaward (major progradational complexes, MPCs) with intercalated sheeted units (widespread sheeted units, WSUs). At least four WSUs have been identified in the seismic records (A to D in descending order). They are in general distributed widely over the shelf and upper slope, although they constitute the bulk of the sedimentary record in the innermost shelf alone and, in places, they

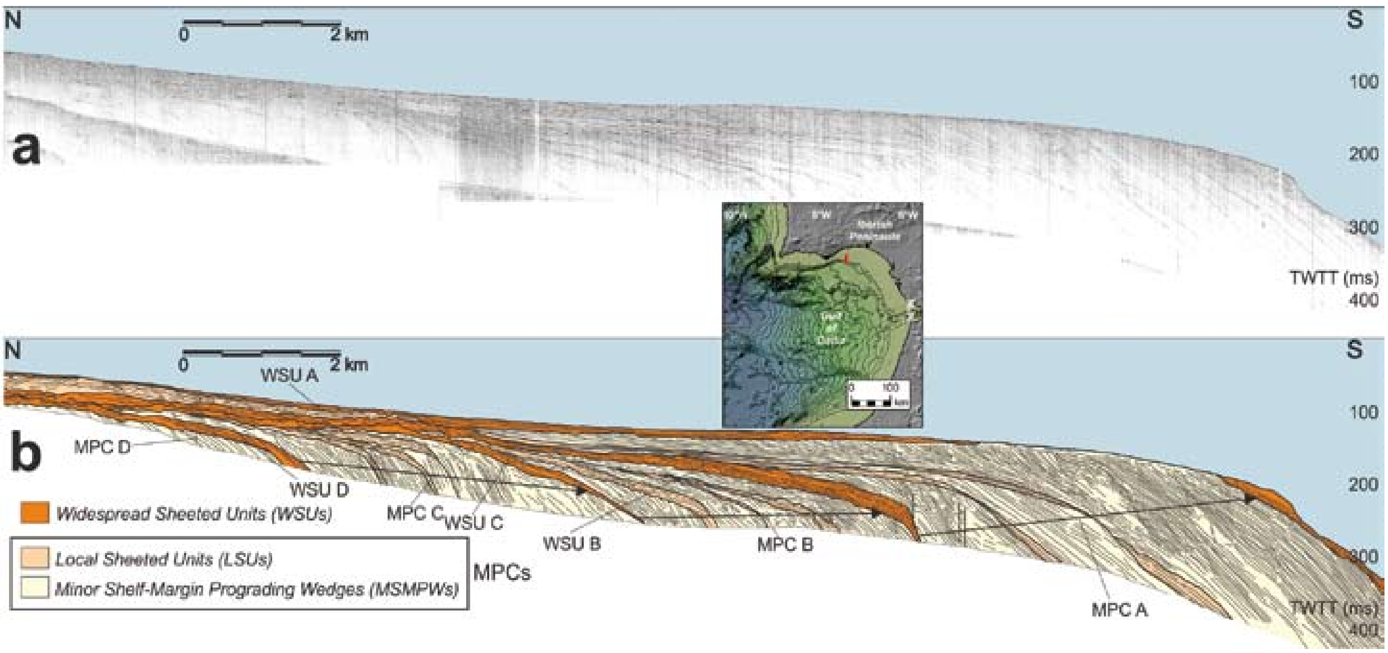

Figure 5. Seismic stratigraphic shelf architecture to the west of the Guadiana River (see position in the location map): (a) Uniboom seismic profile; (b) the stratigraphic pattern is characterized by the alternance of major progradational complexes (MPCs) and widespread sheeted units (WSUs): D to A from older to younger. The MPCs show a more complex internal lower-scale architecture, being composed of an alternance of minor shelf-margin prograding wedges (MSMPWs) and local sheeted units (LSUs).

***Figura 5.** Arquitectura de estratigrafía sísmica de la plataforma al Oeste del Río Guadiana (la posición está indicada en el mapa de localización): (a) perfil sísmico de Uniboom; (b) el patrón estratigráfico está caracterizado por la alternancia de Complejos Progradantes Mayores (MPCs) y Unidades Laminares de Extensión Regional (WSUs), designadas D a A de muro a techo. Internamente, los MPCS muestran una arquitectura de menor escala más compleja, definida por la alternancia de Cuñas Progradantes Menores de Borde de Plataforma (MSMPWs) y Unidades Laminares de Extensión Local (LSUs).*

may thin and pinch out (Fig. 5). Their thickness shows little lateral variability, with values generally ranging between 4-10 m. They are highly dominated internally by sub-parallel, aggrading configurations.

The MPCs pinch out landward in the inner to middle shelf, although in some cases they may also continue landward. The overall thickness of the MPCs increases seaward, although the exact values are difficult to estimate in the seismic profiles due to the ocurrence of multiple reflections (Fig. 5). The most complete record can be seen in MPC A, which is thicker than 100 ms (ca. 75 m) over the palaeo-shelf margin. The internal architecture of the MPCs comprises minor shelf-margin prograding wedges (MSMPWs) which stack laterally to control the margin outbuilding and are separated by local sheeted units (LSUs) (Fig. 5). The MSMPWs generally pinch out landward on the outer palaeo-shelves and vary in thickness, with low values on the palaeo-shelves, which increase abruptly on the upper palaeo-slopes. Alternating LSUs tend to occur on the palaeo-shelves. Most of these LSUs exhibit sub-parallel configurations both in the palaeo-shelf and in the upper palaeo-slope. Their thickness tends to be moderate and constant laterally; some of them are thinner than the WSUs whilst others are just as thick. Their across-shelf distribution, on the other hand, is more limited than that of the WSUs, as they only extend for 2-3 km (Fig. 5).

Sea-level modulation by superimposition of 20 and 100 kyr cycles results in a complex pattern of erosional surfaces separating the progradational deposits composing the bulk of the 100 kyr sequences (Hernández-Molina *et al.*, 2000). It is therefore possible to define smaller scale unconformity-bounded units that can be interpreted as higher-frequency (20 kyr) sequences within each 100 kyr composite sequence (Fig. 6).

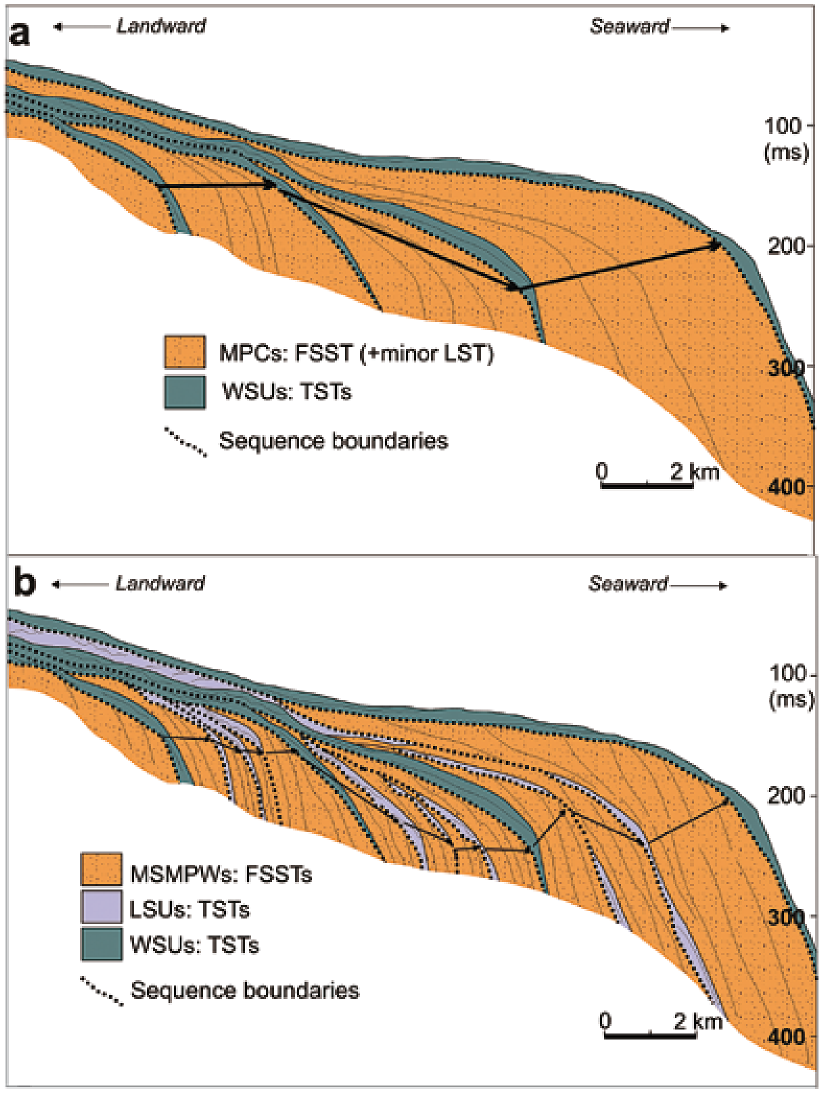

Figure 6. Two scales of stratigraphic architectural variations in the Gulf of Cádiz margin: (a) the large scale is related to 100 kyr cyclicity and is characterized by sheet-like transgressive deposition (widespread sheeted units, WSUs) linked to glacial terminations and wedge-shaped regressive deposition (major progradational complexes, MPCs) related to long-lasting sea-level falls, with erosional truncation associated with the sequence boundaries; (b) the small scale is related to higher frequency climatic variability (20 kyr ?) and is strikingly similar to the large-scale architecture in terms of system tract composition and sequence boundary development, with alternance of transgressive (local sheeted units, LSUs) and regressive deposits (minor shelf-margin progradational wedges, MSMPWs). Arrows indicate shelf-break trajectories which give information about the sense and amount of progradation. Legend: FSST: falling-stage systems tract; LST: lowstand systems tract; TST: transgressive systems tract.

Figura 6. *Dos escalas de variabilidad estratigráfica en el margen del Golfo de Cádiz: (a) la escala de variabilidad mayor se relaciona con la ciclicidad de 100 kyr y se caracteriza por sedimentación transgresiva de láminas sedimentarias (Unidades Laminares de Extensión Regional, WSUs) asociada a las terminaciones glaciares y por sedimentación de cuñas regresivas (Complejos Progradantes Mayores, MPCs) asociada a los descensos prolongados del nivel del mar, con truncaciones erosivas asociadas a la formación de los límites de secuencias; (b) la escala de variabilidad menor se relaciona con una ciclicidad climática de mayor frecuencia (20 kyr?) y muestra una gran similitud con la arquitectura de mayor escala en cuanto a la composición de cortejos sedimentarios y el desarrollo de límites de secuencias, con la alternancia de depósitos transgresivos (Unidades Laminares de Extensión Local, LSUs) y regresivos (Cuñas Progradantes Menores de Borde de Plataforma, MSMPWs). Las flechas indican las trayectorias del borde de plataforma que proporcionan información sobre el sentido y cantidad de progradación. Leyenda: FSST: Cortejo Sedimentario de Descenso del Nivel del Mar; LST: Cortejo Sedimentario de Bajo Nivel del Mar; TST: Cortejo Sedimentario Transgresivo.*

Discussion

Internal architecture of 100 kyr sequences and systems tract distinction

The internal structure of the 100 kyr sequences is relatively uniform and typically consists of internally similar progradational clinoforms recording highstand to lowstand deposition (HST, FSST and LST). In most cases the stratigraphic boundary between HST, FSST and LST progradational units is not evident in the seismic profiles and on this evidence several authors have interpreted the succession of progradational units as representing one single FSST, recording a fall in sea level (Ercilla *et al.*, 1994; Chiocci *et al.*, 1997; Chiocci, 2000; Tesson *et al.*, 2000; Hübscher and Spieß, 2005; Liquete *et al.*, 2008; Maia *et al.*, 2010). As a consequence, increasing efforts have been made to discern the stratigraphic representation of highstands and lowstands associated with interglacial and glacial peaks, which merge with the forced regression units of the falling stage to generate an almost continuous, homogeneous picture of shelf sediment progradation from highstand to lowstand.

A recognition of the boundary between the interglacial HST and the early glacial FSST is essential to an understanding of the sedimentary response to the onset of sea-level fall after a sea-level still stand. HST and early FSST deposits, however, are presumed to be poorly preserved due to sub-aerial erosion during the subsequent sea-level fall (Chiocci *et al.*, 1997). When preserved, the HST-FSST transition seems to be represented by downlap surfaces that record the seaward shift of coastal progradation driven by the sea-level fall; this is stratigraphically marked by upper/proximal FSST clinoform remnants overlying more gentle sigmoid to sub-parallel HST units generated in a more distal shelf environment (Figs 2 and 4). Favourable conditions for the preservation of proximal HST segments would include subsidence rates capable of reducing exposure time and the intensity of sub-aerial and marine erosion by more rapid drowning and burial, as in the case of the Catalonia Shelf (Gámez *et al.*, 2009); sediment supply is also important because high sedimentation rates allow the generation of distal shelf depocentres that survived complete removal during sea-level fall (Browne and Naish, 2003).

Recognition of the FSST-LST boundary is also essential to track the sequence boundaries in the distal shelf margin, an achievement that also proves elusive. Apparently this transition is best recognised in shelf settings where high-angle, coarse-grained lowstand deposits downlap the underlying distal, low-angle progradational clinoforms of the falling stage. Nevertheless, this stratigraphic pattern has been recognised in only a few shelves, such as, for example, the Gulf of Lions (Rabineau *et al.*, 2005), whereas in most cases the FSST-LST transition, marked by the conformable part of the sequence boundary, is masked by concordant reflections of both distal FSSTs and LSTs as well as by the poor development of the LSTs themselves.

In contrast to the extensive deposition and preservation of progradational-regressive units within 100 kyr sequences, the record of transgressive deposits is more variable, ranging from linear/discontinuous tidal or wave-dominated sand ridges to confined/patchy sediment fills or thin regular sheets, which strongly suggest that the amount of terrigenous supply and the type of dispersal systems (wave- versus tide-dominated) pose more constraints on the sedimentary response during sea-level rise. Abrupt sea-level rises are best recorded by the reworking of pre-existing subaerial unconformities, with the major obliteration of evidence of fluvial incision on the shelf (Browne and Naish, 2003). Consequently, transgressive surfaces are the most evident shelf-wide stratigraphic surfaces in the Upper Quaternary record (Figs 3 and 6).

Stratigraphic complexity of 100 kyr sequences: the effect of superimposed 20 kyr cyclicity

In most case studies, either the glacial-interglacial cycle (100 kyr periodicity) or the higher-frequency stadial-interstadial cycle (20 kyr periodicity) has been detected as being dominant in the Upper Quaternary record. In some shallow-water settings, such as the Gulf of Lions, the Adriatic Sea, the Gulf of Cádiz, the Bengal Shelf and the Korea Strait, however, a hierarchical pattern displaying both orders of cycles as distinct stratigraphic motifs has been reported. In these cases the composite pattern is detected within the succession of progradational wedges that records the overall sea-level fall between each interglacial and glacial period. In terms of sequence architecture and systems tracts, this succession has been interpreted by many authors as being the FSST of the 100 kyr sequences. Taking into account the theoretical model of composite cyclicity (Mitchum and Van Wagoner, 1991), progradational units (i.e. 20 kyr motifs) would represent individual sequences that form part of a sequence set (i.e., the FSST of the 100 kyr sequence). Although in the theoretical model smaller scale sequence sets may occur during the entire sea-level cycle, Quaternary sequences display them only within the falling limb of the 100 kyr sea-level curve (Figs 4 and 6). We attribute this marked difference to the asymmetrical pattern exhibited by the 100 kyr cycles during the Late Quaternary; this constrains the interval when the superimposed 20 kyr cycles punctuates the 100 kyr trend within the long-term sea-level falls.

Significance of high-frequency sequences and bounding surfaces

The most common pattern of Quaternary composite 100 and 20 kyr cyclicity is displayed by oblique-tangential clinoforms, each separated by downward-shift surfaces but as a whole forming a major progradational wedge with a strongly forestepping stacking pattern. The clinoform sets bounded by downward-shift surfaces can be interpreted as FSST units, recording single steps of a general sea-level fall within a 100 kyr cycle or, alternatively, as relative LST units deposited after an interval of sea-level drop during each 20 kyr cycle, punctuating the overall 100 kyr sea-level fall. The generation of the downward shift surfaces is related to enhanced submarine erosion during a lowering of the base level concomitant to each sea-level drop (Tesson *et al*., 2000; Yoo *et al*., 2003; Hübscher and Spieß, 2005).

Our datasets from the Gulf of Cádiz and the Adriatic Sea reveal significant departures from the theoretical prediction of composite cyclicity records (*c.f.* Mitchum and van Wagoner, 1991). Moreover, the Gulf of Cádiz and Adriatic examples show differences both in terms of the nature of their bounding surfaces and overall clinoform pattern of their 20 kyr units. These differences would indicate that regional subsidence, sediment supply and dispersal can profoundly modify the stratigraphic expression of 20 kyr cycles superimposed upon, though in a subdued way, the 100 kyr pacing that controls the origin of the main sequence boundaries and sequences in Quaternary margins.

In the Gulf of Cádiz the 20 kyr architectural pattern differs from that of other margins in the following ways (Fig. 6): (a) the shape of regressive wedges, which in the Gulf of Cádiz (i.e., MSMPWs) show seaward thickening and preservation of proximal facies, whereas in other settings the shape of regressive wedges reflects seaward-thinning; (b) the presence in the Gulf of Cádiz of sheet deposits recording transgressive intervals, which are apparently missing in other settings; (c) the preservation in the Gulf of Cádiz of a shelf margin marked by top-lap geometry, which confers an overall convex morphology to sequence boundaries, in contrast with other settings where exclusively erosional, concave-up bounding surfaces prevail. These differences [particularly (a) and (b)] possibly reflect conditions of increased sediment supply enhancing the preservation of the small-scale architecture. Because of this higher preservation potential, the proximal segments of progradational units and part of the interposed erosional unconformity are also preserved, thus allowing a sequence boundary to be traced at the 20 kyr unit scale. Therefore, and in contrast to other settings where surfaces separating progradational units appear as the product of submarine erosion (e.g. the Adriatic margin), these units show an essential prerequisite for being interpreted as belonging to a 5th order depositional sequence.

In the Adriatic shelf, variations in the shape (geometry and thickness of bottomsets) of HST and FSST progradational units within 100 kyr sequences is the most evident stratigraphic signature of the superimposed 20 kyr cyclicity (Fig. 4). These variations reflect different patterns of fine-sediment dispersal during alternating highstand (interglacial/interstadial) and falling (stadial) or lowstand (glacial) sea-level conditions, with highstands characterised by more efficient advection, enhancing the distal growth of progradational clinoforms.

Although a sea-level rise is associated with the onset of successive high-frequency HSTs, the corresponding TST deposits are difficult to separate from the HST because their limit, based on isotope stratigraphy, does not correspond to any key reflector traceable across the slope and shelf. The only transgressive deposits that attain significant thickness and can be more firmly constrained (especially within the younger sequence 1) are those recording major terminations (Ridente *et al*., 2008). With these limitations, the two types of alternating clinoforms recording deposition from MIS 5.5 to MIS 4-2 within sequence 1 are regarded as encompassing TST/HST and FSST/LST deposits at the 20 kyr cyclicity scale. A similar pattern is shown by units of sequence 2, formed during MIS 7, and by units of sequence 3, formed during MIS 9 (Figs 1 and 2).

These results indicate that the expression of 20 kyr cycles in the Adriatic is not that of smaller scale sequences, each bounded by smaller-scale sequence boundaries (as in the Gulf of Cádiz), but rather reflects the impact of 20 kyr sea-level changes upon sediment dispersal dynamics, ultimately controlling the geometry and shape of shelf clinoforms. The Adriatic example suggests that perhaps on other continental margins as well the expression of 20 kyr sequences may reflect the bias of local environmental factors rather than the direct control of sea-level oscillations. More in general, because sea level and local factors interplay in diverse ways, the key for resolving the 20 kyr sequences may not be provided by any general model such as sequence stratigraphy.

Conclusions

The long known difficulty encountered in defining the sedimentary record of both the 100 and 20 kyr cycles of the Late Quaternary sea-level curve and thus unravelling the composite nature of sequences building most terrigenous margins can be addressed in shelf settings where sediment supply, dispersal dynamics and subsidence regime concur to favour the generation and preservation of discrete units (i.e. sequences and systems tracts) reflecting both scales of cyclicity.

Depositional sequences responding to 100 kyr pacing occur as sets of unconformity-bounded sequences; the unconformity is a polygenic (sub-aerial and marine) erosional surface, ultimately recording transgressive ravinement. 100 kyr sequences display a typical internal motif of several similar progradational wedges overlying stratigraphically less continuous and more heterogeneous transgressive deposits. Despite the fact that the sequence stratigraphy model claims that sequences at different scales (i.e. order of cyclicity) invariably display a basic fractal pattern in their architecture, evidence for this is not unambiguously provided by the Quaternary composite 100 and 20 kyr cycles. In fact, in contrast to the more uniform representation of 100 kyr sequences, stratigraphic architectures resulting from the 20 kyr cyclicity show a highly variable representation both in space (i.e. along with systems-tract partitioning) and in time (with changes in the nature of depositional systems). This holds particularly true for the nature of surfaces bounding 20 kyr units, which remain as erosional unconformities in some settings, thus allowing 20 kyr sequences to be defined, whereas in others they correspond to marine depositional surfaces that merely mark the limits between the different systems tracts of the 100 kyr sequence. Finally, data from the literature and the in-depth analysis based on the two case studies (covering at least the past 500 kyr) highlight the lack of evidence for any stratigraphic pattern that could be referred to as a signature of the 40 kyr obliquity cycle.

Acknowledgements

This paper was completed thanks to the support of the research project CGL2011-30302-C02-02, from the Spanish R+D Program. Numerous suggestions to improve the original version of the manuscript were provided by Jaume Dinarès-Turell and by an anonymous reviewer.

References

Abdulah, K.C., Anderson, J.B., Snow, J.N. and Holdford-Jack, L. 2004. The Late Quaternary Brazos and Colorado deltas, offshore Texas, U.S.A. — Their evolution and the factors that controlled their deposition. In: Anderson, J.B. and Fillon, R.H. (Eds.), *Late Quaternary Stratigraphic Evolution of the Northern Gulf of Mexico Margin, SEPM Special Publication*, 79, 237-269.

Ashley, G.M., Wellner, R.W., Esker, D. and Sheridan, R.E., 1991. Clastic sequences developed during late Quaternary glacio-eustatic sea-level fluctuations on a passive margin: Example from the inner continental shelf near Barnegat Inlet, New Jersey. *Geological Society of America Bulletin*, 103(12), 1607-1621.

Banfield, L.A. and Anderson, J.B. 2004. Late Quaternary evolution of the Rio Grande delta: complex response to eustasy and climate change. In: Anderson, J.B. and Fillon, R.H. (Eds.), *Late Quaternary Stratigraphic Evolution of the Northern Gulf of Mexico Margin, SEPM Special Publication*, 79, 289-306.

Bard, E., Hamelin, B. and Fairbanks, R.G. 1990. U-Th ages obtained by mass spectrometry in corals from Barbados: sea level during the past 130 000 years. *Nature*, 346(6283), 456-458.

Bassetti, M.A., Berné, S., Jouet, G., Taviani, M., Dennielou, B., Flores, J.A., Gaillot, A., Gelfort, R., Lafuerza, S. and Sultan, N., 2008. The 100-ka and rapid sea level changes recorded by prograding shelf sand bodies in the Gulf of Lions (western Mediterranean Sea). *Geochemistry Geophysics Geosystem*s, 9(11), Q11R05.

Bellec, V.K. and Cirac, P., 2010. Internal architecture of the soft sediment cover of the South-Aquitaine shelf (Bay of Biscay): A record of high frequency sea level variations?. *Comptes Rendus Geosciences*, 342(1), p. 79-86.

Berné, S., Vagner, P., Guichard, F., Lericolais, G., Liu, Z., Yin, P., Trentesaux, A. and Yi, H.I. 2002. Pleistocene forced-regressions and tidal sand ridges in the East China Sea. *Marine Geology*, 188(3-4), 293-315.

Bloom, A.L., Broecker, W.S., Chappell, J.M.A., Matthews, R.K. and Mesolella, K.J. 1974. Quaternary sea level fluctuations on a tectonic coast: New $^{230}Th/^{234}U$ dates from the Huon Peninsula, New Guinea. *Quaternary Research*, 4(2), 185-205.

Browne, G.H. and Naish, T.R., 2003. Facies development and sequence architecture of a late Quaternary fluvial-marine transition, Canterbury Plains and shelf, New Zealand: implications for forced regressive deposits. Sedimentary Geology, 158(1-2), 57-86.

Burger, R.L., Fulthorpe, C.S., Austin, J.A. and Gulick, S.P.S. 2002. Lower Pleistocene to present structural deformation and sequence stratigraphy of the continental shelf, offshore Eel River Basin, northern California. *Marine Geology*, 185(3-4), 249-281.

Çağatay, M.N., Eris, K., Ryan, W.B.F., Sancar, Ü., Polonia, A., Akçer, S., Biltekin, D., Gasperini, L., Görür, N., Lericolais, G. and Bard, E. 2009. Late Pleistocene-Holocene evolution of the northern shelf of the Sea of Marmara. *Marine Geology*, 265(3-4), 87-100.

Cattaneo, A., Correggiari, A., Langone, L. and Trincardi, F. 2003. The late-Holocene Gargano subaqueous delta, Adriatic shelf: Sediment pathways and supply fluctuations. *Marine Geology*, 193(1-2), 61-91.

Chappell, J., Omura, A., Esat, T., McCulloch, M., Pandolfi, J., Ota, Y. and Pillans, B. 1996. Reconciliation of late Quaternary sea levels derived from coral terraces at Huon Peninsula with deep sea oxygen isotope records. *Earth and Planetary Science Letters*, 141(1-4), 227-236.

Chiocci, F.L. 2000. Depositional response to Quaternary fourth-order sea-level fluctuations on the Latium margin (Tyrrhenian Sea, Italy). In: Hunt, D. and Gawthorpe, R.L. (Eds.), *Sedimentary Responses to Forced Regressions. Geological Society Special Publication*, 172, 271-289.

Chiocci, F.L., Ercilla, G. and Torres, J., 1997. Stratal architecture of Western Mediterranean Margins as the result of the stacking of Quaternary lowstand deposits below 'glacio-eustatic fluctuation base-level'. *Sedimentary Geology*, 112(3-4), 195-217.

Cronin, T.M. 1983. Rapid sea level and climate change: Evidence from continental and island margins. *Quaternary Science Reviews*, 1(3), 177-214.

Cutler, K.B., Edwards, R.L., Taylor, F.W., Cheng, H., Adkins, J., Gallup, C.D., Cutler, P.M., Burr, G.S. and Bloom, A.L. 2003. Rapid sea-level fall and deep-ocean temperature change since the last interglacial period. *Earth and Planetary Science Letters*, 206(3-4), 253-271.

Emiliani, C. 1955. Pleistocene temperatures. *The Journal of Geology*, 63(6), 538–578.

Ercilla, G., Farrán, M., Alonso, B. and Díaz, J.I., 1994. Pleistocene progradational growth pattern of the northern Catalonia continental shelf (northwestern Mediterranean). Geo-Marine Letters, 14(4), 264-271.

Gallup, C.D., Edwards, R.L. and Johnson, R.G. 1994. The Timing of High Sea Levels Over the Past 200 000 Years. *Science*, 263(5148), 796-800.

Gámez, D., Simó, J.A., Lobo, F.J., Barnolas, A., Carrera, J. and Vázquez-Suñé, E. 2009. Onshore-offshore correlation of the Llobregat deltaic system, Spain: Development of deltaic geometries under different relative sea-level and growth fault influences. *Sedimentary Geology*, 217(1-4), 65-84.

Hanebuth, T.J., Stattegger, K. and Saito, Y. 2002. The stratigraphic architecture of the central Sunda Shelf (SE Asia) recorded by shallow-seismic surveying. *Geo-Marine Letters*, 22(2), 86-94.

Hays, J.D., Imbrie, J. and Shackleton, N.J. 1976. Variations in the Earth's Orbit: Pacemaker of the Ice Ages. *Science*, 194(4270), 1121–1132.

Hernández-Molina, F.J., Somoza, L. and Lobo, F. 2000. Seismic stratigraphy of the Gulf of Cádiz continental shelf: a model for Late Quaternary very high-resolution sequence stratigraphy and response to sea-level fall. In: Hunt, D. and Gawthorpe, R.L.G. (Eds.), *Sedimentary Responses to Forced Regressions, Geological Society, London, Special Publication*, 172, 329-362.

Hiscott, R.N. 2001. Depositional sequences controlled by high rates of sediment supply, sea-level variations, and growth faulting: the Quaternary Baram Delta of northwestern Borneo. *Marine Geology*, 175(1-4), 67-102.

Hübscher, C. and Spieß, V., 2005. Forced regression systems tracts on the Bengal Shelf. *Marine Geology*, 219(4), 207-218.

Imbrie, J., Hays, J.D., Martinson, D.G., McIntyre, A., Mix, A.C., Morley, J.J., Pisias, N.G., Prell, W.L. and Shackleton, N.J., 1984. The orbital theory of Pleistocene climate: support from a revised chronology of the marine $\delta^{18}O$ record. In: Berger, A.L., Hays, J., Imbrie, J., Saltzman, B., and Kukla, G.J. (Eds.), *Milankovitch and climate, Part 1, Volume 1*: Palisades, Reidel Publishing Company, p. 269-305.

Imbrie, J., Berger, A., Boyle, E.A., Clemens, S.C., Duffy, A., Howard, W.R., Kukla, G., Kutzbach, J., Martinson, D.G., McIntyre, A., Mix, A.C., Molfino, B., Morley, J.J., Peterson, L.C., Pisias, N.G., Prell, W.L., Raymo, M.E., Shackleton, N.J. and Toggweiler, J.R. 1993. On the structure and origin of major glaciation cycles. II. The 100 000-year cycle. *Paleoceanography*, 8(6), 699–735.

Jin, J.H., Chough, S.K. and Ryang, W.H., 2002. Sequence aggradation and systems tracts partitioning in the mid-eastern Yellow Sea: roles of glacio-eustasy, subsidence and tidal dynamics. *Marine Geology*, 184, 249-271.

Kitamura, A., Matsui, H. and Oda, M. 2000. Constraints on the timing of systems tract development with respect to sixth-order (41 ka) sea level changes: an example from the Pleistocene Omma Formation, Sea of Japan. *Sedimentary Geoleology*, 131(1-2), 67–76

Kolla, V., Biondi, P., Long, B. and Fillon, R., 2000. Sequence stratigraphy and architecture of the Late Pleistocene Lagniappe delta complex, northeast Gulf of Mexico. In: Hunt, D., and Gawthorpe, R.L. (Eds.), *Sedimentary Responses to Forced Regressions, Geological Society, London, Special Publication*, 172, 291-327.

Labeyrie, L.D., Duplessy, J.C. and Blanc, P.L., 1987. Variations in mode of formation and temperature of oceanic deep waters over the past 125 000 years. *Nature*, 327(6122), 477–482.

Lea, D.W., Martin, P.A., Pak, D.K. and Spero, H.J. 2002. Reconstructing a 350 ky history of sea level using planktonic Mg/Ca and oxygen isotope records from a Cocos Ridge core. *Quaternary Science Reviews*, 21(1-3), 283-293.

Liquete, C., Canals, M., De Mol, B., De Batist, M. and Trincardi, F. 2008. Quaternary stratal architecture of the Barcelona prodeltaic continental shelf (NW Mediterranean). *Marine Geology*, 250(3-4), 234-250.

Liu, J., Saito, Y., Kong, X., Wang, H., Wen, C., Yang, Z. and Nakashima, R. 2010. Delta development and channel incision during marine isotope stages 3 and 2 in the western South Yellow Sea. *Marine Geology*, 278(1-4), 54-76.

Liu, Z.-X., Berné, S., Saito, Y., Lericolais, G. and Marsset, T. 2000. Quaternary seismic stratigraphy and paleoenvironments on the continental shelf of the East China Sea. *Journal of Asian Earth Sciences*, 18(4), 441-452.

Lobo, F.J., Hernandez-Molina, F.J., Somoza, L., Dıaz del Rıo, V. and Dias, J.M.A. 2002. Stratigraphic evidence of an upper Pleistocene TST to HST complex on the Gulf of Cádiz continental shelf (south-west Iberian Peninsula). *Geo-Marine Letters*, 22(2), 95-107.

Maia, R.M.d.C., Reis, A.T.d., Alves, E.d.C., Silva, C.G., Guerra, J.V., Gorini, C., Silva, A. and Arantes-Oliveira, R., 2010. Architecture and stratigraphic framework of shelf sedimentary systems off Rio de Janeiro state, Northern Santos Basin-Brazil. *Brazilian Journal of Oceanography*, 58(SI 1), 15-29.

Marsset,T., Xia, D., Berné, S., Liu, Z., Bourillet, J.-F. and Wang, K. 1996. Stratigraphy and sedimentary environments during the Late Quaternary, in the Eastern Bohai Sea (North China Platform). *Marine Geology*, 135(1-4), 97-114.

Martinson, D.G., Pisias, N.G., Hays, J.D., Imbrie, J., Moore, T.C. and Shackleton, N.J. 1987. Age dating and the orbital theory of the ice ages: development of a high-resolution 0 to 300 000-year chronostratigraphy. *Quaternary Research*, 27(1), 1-29.

Massari, F., Sgavetti, M., Rio, D., D'Alessandro, A. and Prosser, G. 1999. Composite sedimentary record of falling stages of Pleistocene glacio-eustatic cycles in a shelf setting (Crotone basin, south Italy). *Sedimentary Geology*, 127(1-2), 85-110.

McHugh C.M.G. and Olson, H.C. 2002. Pleistocene chronology of continental margin sedimentation: New insights into traditional models, New Jersey. *Marine Geology*, 186(3-4), 389-411.

Milankovitch, M. 1930. Matematische klimalehre und astronomische theorie der klimaschwankungen, In: Köppen, W. and Geiger, R. (Eds.), *Hanbuch der klimatologie*, I (A). Berlin, Gebrüder Borntraeger, 1–176.

Mitchum, R.M.J. and Van Wagoner, J.C. 1991. High-frequency sequences and their stacking patterns: sequence-stratigraphic evidence of high-frequency eustatic cycles. *Sedimentary Geology*, 70(2-4), 131-160.

Naish, T. and Kamp, P.J.J. 1997. Sequence stratigraphy of sixth-order (41 k.y.) Pliocene-Pleistocene cyclothemes, Wanganui basin, New Zealand: a case for the regressive systems tract. *Geological Society of America Bulletin*, 109(8), 978–999.

Osterberg, E.C. 2006. Late Quaternary (marine isotope stages 6-1) seismic sequence stratigraphic evolution of the Otago continental shelf, New Zealand. *Marine Geology*, 229(3-4), 159-178.

Petit, J. R., Jouzel, J., Raynaud, D., Barkov, N. I., Barnola, J.-M., Basile, I., Bender, M., Chappellaz, J., Davis, M., Delaygue, G., Delmotte, M., Kotlyakov, V. M., Legrand, M., Lipenkov, V. Y., Lorius, C., Pépin, L., Ritz, C., Saltzman, E. and Stievenard M. 1999. Climate and atmospheric history of the past 420 000 years from the Vostok ice core, Antarctica. *Nature*, 399(6735), 429-436.

Piper, D.J.W. and Aksu, A.E. 1992. Architecture of stacked Quaternary deltas correlated with global oxygen isotopic curve. *Geology*, 20(5), 415-418.

Plint, A.G. 1991. High-frequency relative sea-level oscillations in the Upper Cretaceous shelf clastics of the Alberta foreland basin: possible evidence for glacio-eustatic control? In: Macdonald, D.I.M. (Ed.), *Sedimentation, Tectonics and Eustasy*, *IAS Special Publication*, 12, 409-428.

Rabineau, M., Berné, S., Aslanian, D., Olivet, J.L., Joseph, P., Guillocheau, F., Bourillet, J.F., Le Drezen, E. and Grangeon, D. 2005. Sedimentary sequences in the Gulf of Lion: a record of 100 000 years climatic cycles. *Marine and Petroleum Geology*, 22(6-7), 775-804.

Raymo, M.E., Oppo, D. W. and Curry, D.W. 1997. The mid-Pleistocene climate transition: A deep sea carbon isotopic perspective. *Paleoceanography*, 12(4), 546–559.

Ridente, D. and Trincardi, F. 2005. Pleistocene "muddy" forced-regression deposits on the Adriatic shelf: a comparison with prodelta deposits of the late Holocene highstand mud wedge. *Marine Geology*, 222-223 (Mediterranean Prodelta Systems), 213-233.

Ridente, D., Trincardi, F., Piva, A., Asioli, A. and Cattaneo, A. 2008. Sedimentary response to climate and sea level changes during the past ~ 400 ka from borehole PRAD1-2 (Adriatic margin). *Geochemistry Geophysics Geosystems*, 9(Q09R04).

Ridente, D., Petrungaro, R., Falese, F. and Chiocci, F.L. 2012. Middle-Upper Pleistocene record of 100 ka cycles on the Southern Tuscany continental margin (Tyrrhenian Sea, Italy). Sequence architecture and margin growth pattern. *Marine Geology*, 326-328, 1-13.

Rohling, E.J., Fenton, M., Jorissen, F.J., Bertrand, P., Ganssen, G. and Caulet, J.P. 1998. Magnitudes of sea-level lowstands of the past 500 000 years. *Nature*, 394(6689), 162-165.

Ruddiman, W.F. 2003. Orbital insolation, ice volume, and greenhouse gases. *Quaternary Science Reviews*, 22(15-17), 1597-1629.

Shackleton, N.J. 1987. Oxygen isotopes, ice volume and sea level. *Quaternary Science Reviews*, 6(3-4), 183-190.

Shackleton, N.J. 1997.The deep-sea sediment record and the Plio-Pleistocene boundary. *Quaternary International*, 40, 33-35.

Shackleton, N.J. 2000. The 100 000-Year Ice-Age Cycle Identified and Found to Lag Temperature, Carbon Dioxide, and Orbital Eccentricity. *Science*, 289(5486), 1897-1902.

Shackleton, N.J. and Opdyke, N.D. 1973. Oxygen isotope and palaeomagnetic stratigraphy of equatorial Pacific core V28–238: oxygen isotope temperature and ice volumes on a 105 and 106 year scale. *Quaternary Research*, 3(1), 39–59.

Siddall, M., Rohling, E.J., Almogi-Labin, A., Hemleben, C., Meischner, D., Schmelzer, I. and Smeed, D.A. 2003. Sea-level fluctuations during the last glacial cycle. *Nature*, 423(6942), 853-858.

Siddall, M., Chappell, J. and Potter, E.K. 2007. Eustatic sea level during past interglacials. In: Sirocko, F., Claussen, M., Sánchez-Goñi, M.F. and Litt, T. (Eds.), *The Climate of Past Interglacials*, *Developments in Quaternary Sciences*, 7, 75-92.

Siddall, M., Kaplan, M.R., Schaefer, J.M., Putnam, A., Kelly, M.A. and Goehring, B. 2010. Changing influence of Antarctic and Greenlandic temperature records on sea-level over the last glacial cycle. *Quaternary Science Reviews*, 29(3-4), 410-423.

Somoza, L., Hernández-Molina, F.J., De Andrés, J.R. and Rey, J. 1997. Continental shelf architecture and sea-level cycles: Late Quaternary high-resolution stratigraphy of the Gulf of Cádiz, Spain. *Geo-Marine Letters*, 17(2), 133-139.

Steckler, M.S., Ridente, D. and Trincardi, F. 2007. Modeling of sequence geometry north of Gargano Peninsula by changing sediment pathways in the Adriatic Sea. *Continental Shelf Research*, 27(3-4), 526-541.

Sydow, J. and Roberts, H.H. 1994. Stratigraphic framework of late Pleistocene shelf-edge delta, Northeast Gulf of Mexico. *AAPG Bulletin*, 78(8), 1276-1312.

Tesson, M., Posamentier, H.W. and Gensous, B. 2000. Stratigraphic organization of late Pleistocene deposits of the western part of the Golfe du Lion shelf (Languedoc shelf), western Mediterranean Sea, using high-resolution seismic and core data. *AAPG Bulletin*, 84(1), 119-150.

Trincardi, F. and Correggiari, A. 2000. Quaternary forced-regression deposits in the Adriatic basin and the record of composite sea-level cycles. In: Hunt, D. and Gawthorpe, R.L. (Eds.), *Sedimentary Responses to Forced Regressions, Geological Society Special Publication*, 172, 245-269.

Ulug, A., Duman, M., Ersoy, S., Özel, E. and Avci, M. 2005. Late Quaternary sea-level change, sedimentation and neotectonics of the Gulf of Gökova: Southeastern Aegean Sea. *Marine Geology*, 221(1-4), 381– 395.

Vail, P.R., Mitchum, R.M. and Sangree, J.B. 2002. Concepts of Depositional Sequences. In: Armentrout, J. (Ed.), *Sequence Stratigraphic Models for Exploration and Production: Evolving Methodology, Emerging Models, and Application Histories: 22nd Annual. GCSSEPM Foundation Annual Bob F. Perkins Research Conference Proceedings*, 22, 19-32.

Waelbroeck, C., Labeyrie, L., Michel, E., Duplessy, J.C., McManus, J.F., Lambeck, K., Balbon, E. and Labracherie, M. 2002. Sea-level and deep water temperature changes derived from benthic foraminifera isotopic records. *Quaternary Science Reviews*, 21(1-3), 295-305.

Williams, D.F., Moore, W.S. and Fillon, R.H. 1981. Role of glacial Arctic Ocean ice sheets in Pleistocene oxygen isotope and sea level records. *Earth and Planetary Science Letters*, 56, 157-166.

Yokoyama, Y. and Esat, T.M. 2011. Global climate and sea level: Enduring variability and rapid fluctuations over the past 150 000 years. *Oceanography*, 24(2), 54-69.

Yoo, D.-G. and Park, S.-C. 2000. High-resolution seismic study as a tool for sequence stratigraphic evidence of high-frequency sea-level changes: Latest Pleistocene-Holocene example from the Korea Strait. *Journal of Sedimentary Research*, 70(2), 296-309.

Yoo, D.-G., Park, S.-C., Sunwoo, D. and Oh, J.-H., 2003. Evolution and chronology of late pleistocene shelf-perched lowstand wedges in the Korea strait. *Journal of Asian Earth Sciences*, 22(1), 29-39.

Recibido: octubre 2012
Revisado: noviembre 2012
Aceptado: diciembre 2012
Publicado: abril 2013